

THE EFFECT OF LASER SCAN STRATEGY ON DISTORTION AND RESIDUAL STRESSES OF ARCHES MADE WITH SELECTIVE LASER MELTING

Stacey D. Bagg¹, Lindsay M. Sochalski-Kolbus², and Jeffrey R. Bunn²

¹Metal Joining and Processes

NASA Marshall Space Flight Center
Huntsville, AL, USA

²Chemical and Engineering Materials Division
Oak Ridge National Laboratory
Oak Ridge, TN, USA

COPYRIGHT NOTICE

A portion of this research used resources at the High Flux Isotope Reactor, a DOE Office of Science User Facility operated by the Oak Ridge National Laboratory

INTRODUCTION

The NASA Marshall Space Flight Center (MSFC) is developing Additive Manufacturing (AM) - both in-space AM for on-demand parts, tools, or structures, and on-earth AM for rapid, reduced-cost, small volume production of complex space-flight hardware. Selective Laser Melting (SLM) is an on-earth AM technology that MSFC is using to build Alloy 718 rocket engine components. An understanding of the SLM-718 material properties is required to design, build, and qualify these components for space flight. Residual stresses and are of particular interest for this AM process, since SLM is a series of ~100 μm -wide welds, where highly non-linear heating and cooling, severe thermal gradients and repeated thermal cycling can result in high residual stresses within the component. These stresses may cause degraded material properties, and warp or distort the geometry of the SLM component. The distortions can render the component out-of-tolerance when inspected, and even interrupt or halt the build process if the warped material prevents the SLM machine from operating properly. The component must be scrapped and re-designed, which is time consuming and costly. If residual stresses are better understood, and can be predicted, these effects can be mitigated early in the component's design.

Researchers at the ORNL Neutron Residual Stress Facility (NRSF) have conducted volumetric residual stress measurements on basic shapes of Alloy 718 – through work with

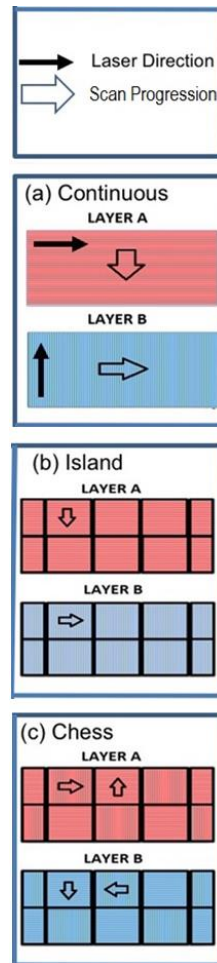


FIGURE 1.
Scanning
Strategies

NASA, Honeywell, the ORNL Manufacturing Demonstration Facility (MDF), and others. This work found that laser-based systems (such as SLM) generate significantly higher residual stresses than electron-beam systems [1], so this is a critical area to address for the SLM technology in particular. This concern is underscored by research that has found residual stresses in excess of 2x the wrought material yield stress in 316L manufactured with SLM [2].

The laser scan and hatching strategy was hypothesized to have an effect on residual stresses, based on the work of Mercelis and Kruth [3] [4]. The common "continuous" scan uses a back-and-forth hatching pattern along the entire dimension of the part in the direction that the laser is scanning. Strategies to reduce residual stresses (proposed by Kruth and his collaborators [3] [4]) segment the layer pattern

into 5 mm x 5 mm squares which are melted in a non-sequential pattern to minimize heat build-up. Concept Laser GmbH, the equipment manufacturer for the SLM

machine used in this research, adopted two versions of this strategy - “chess” and “island,” These are shown and described in Fig. 1. This research investigated the effect of these strategies on component deformations and volumetric residual stresses.

BACKGROUND STUDY

An initial study (Bagg, Kolbus and Babu, unpublished) has shown that laser scan strategy has an effect on residual stress, but not in the predicted way – the chess and island strategies designed to minimize stresses actually showed higher stress than continuous scanning in small (20 mm x 10 mm x 6.5 mm) rectangular prism samples. Scanning strategies and component orientations were held identical to the current study, and are described in the Experimental section. Very low stresses were measured in the x-direction for all samples. In the y-direction, compressive stress was seen at the center of the samples. The average stress in the chess pattern was -132 MPa, compared with island at -118 MPa and continuous at -122 MPa. Tensile stress was exhibited in the top layer of the chess sample in the y-direction, which was absent in the other two samples. Tensile stress was seen in the z-direction at the center of the sample for all samples, again with chess averaging the highest magnitude (128 MPa), followed by island (112 MPa) then continuous (97 MPa). Some compressive stress was seen in the z-direction at the corners of the samples on the top layer, with chess netting the highest magnitude. ORNL and NASA continued to expand on this work, and the study described by this extended abstract was conducted to check the results of the previous work and investigate whether this finding applies to more complex components.

The samples in the initial study were cut off the build plate prior to neutron residual stress measurement which relieved stresses that a component would experience during the build. A build interruption approximately half way through the build led to higher stresses near the mid-height of the build rather than the predicted high tensile stresses at the top of the build that have been witnessed in other research [1] [2] [5]. To address these uncertainties, this study investigated the relaxation effect of cutting the components off of the build plate, and was controlled to prevent build interruptions.

An additional feature of this present study was the investigation into build distortions.

Distortions are coupled with residual stresses – if a part has higher stresses, it will deform more if it is not constrained. The hypothesis resulting from the initial study was that the binding between segments did not allow the chess pattern to deform, leading to higher residual stresses – this would also explain why the chess strategy is preferred by machine operators due to it generating less warpage and fewer build interruptions.

EXPERIMENTAL

Sample Preparation

The sample geometry was selected to duplicate a geometry used by Dr. Kruth [3] to investigate residual stresses in SLM through measurement of distortion in an arch. By utilizing an identical sample geometry, results can be compared with Dr. Kruth's. The geometry is shown in Fig. 1.

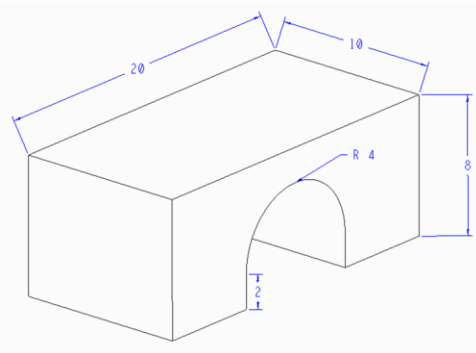


FIGURE 2. Sample Geometry

The SLM process parameters and laser scanning patterns were selected to be identical to the study described in the Background section. These were consistent with parameters used by NASA for printing Alloy 718, shown in Table 1.

Three duplicates of each sample (A, B, and C) were printed on to a 90 mm x 90 mm stainless steel build plate. The Concept Laser SLM scans at +45° and -45° so the samples were oriented at 45° to align the scan hatches with the major axes of the samples, as shown in Fig. 1. After initial surface profilometry measurements, the baseplate was cut into three sections (shown in Fig. 3) and samples were cut off of the two corner sections. All samples were again measured with the profilometer, to investigate distortion from the stresses relieving.

TABLE 1. Sample SLM Parameters

Material	Alloy 718 Powder, 10-45 μm
Layer Thickness	0.030 mm
Laser Power	180 W
Laser Speed	600 mm/s
Hatch Width	0.105 mm
Island Geometry	5 mm x 5 mm squares Overlapping by 0.0225 mm on each side Offset by 1 mm in x and y for each layer
Scan Strategy "A"	Continuous
Scan Strategy "B"	Island
Scan Strategy "C"	Chess

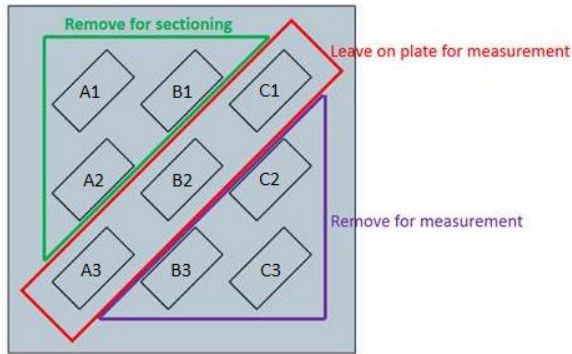


FIGURE 3. Baseplate Configuration

Profilometer Measurements

Non-contact point light profilometry was conducted on the top surface of each component before and after being cut from the build plate. This allowed researchers to characterize the distortion resulting from stress relaxation after the baseplate constraint was eliminated. A Solarius Development Corporation LaserScan was used. This custom profilometer used a Stil CCS Prima chromatic confocal sensor (CCS) paired with a WLC4 optical pen and Optima controller, resulting in a white light CCS which has a 2.5 mm range and 130 nm z-resolution. A 200 mm XY air bearing stage allowed spatial maps to be collected over the surfaces.

Data analysis included leveling over the entire surface using least square plane, and thresholding to remove outlier data where slopes on the rough AM surface exceeded the $\pm 22^\circ$ limit of the CCS. A 3-D plot of the surface was generated for evaluation. A line profile along the

center of each sample was taken from the surface data, and form removal was used to evaluate the curvature of the distorted samples.

Volumetric Residual Stress Measurement

Neutron diffraction at the ORNL High Flux Isotope Reactor (HFIR) NRSF2 was used to measure lattice spacing (d_{hkl}) in the x, y and z planes at the spatially mapped locations shown in Fig. 4 for the purpose of strain calculation. In addition to the experimental samples, lattice spacing on one sectioned sample was measured for a stress-free reference. A gauge volume of 2 mm³ was selected, as it allowed sufficient points for a spatial map while incorporating enough grains for a reliable measurement [6] and assuring gauge volume burial (a partial gauge volume introduces a peak shift that can be mistaken for strain [7], so full gauge volume burial is critical).

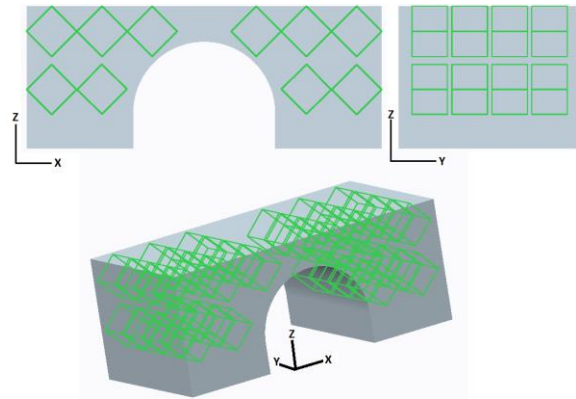


FIGURE 4. Spatially Mapped Gauge Volumes shown in Sample

Residual strain was calculated in the sample x, y and z directions, assuming these to be the principal axes (shear strains are zero). Strain is calculated from the difference in measured interplanar lattice spacing d_{hkl} from the stress-free reference spacing d_{hkl}^0 , shown in Equation 1.

$$\varepsilon_{hkl} = \frac{d_{hkl} - d_{hkl}^0}{d_{hkl}^0} \quad \text{EQUATION 1}$$

Residual stress was then determined using Hooke's law, Equation 2.

$$\sigma_a = \frac{E}{(1 + \nu)(1 - 2\nu)} [\varepsilon_a(1 - \nu) + \nu(\varepsilon_b + \varepsilon_c)] \quad \text{EQUATION 2}$$

This calculation is conducted for the three assumed principal directions, leading to determinations of σ_{xx} , σ_{yy} and σ_{zz} .

RESULTS

Profilometer Measurements

All three samples bowed after removal, as predicted through the use of the arch geometry, and the Solaris LaserScan measurements revealed the highest distortion in the chess sample (shown in Fig. 5). Although the distorted shape exaggerates the raised edges, these are an artifact of the SLM process and not distortion after removal – they can be seen in the pre-removal data as well. Thus a fairly symmetric bowing is observed along the x-dimension of the sample, and a centerline profile can be used to characterize the shape.

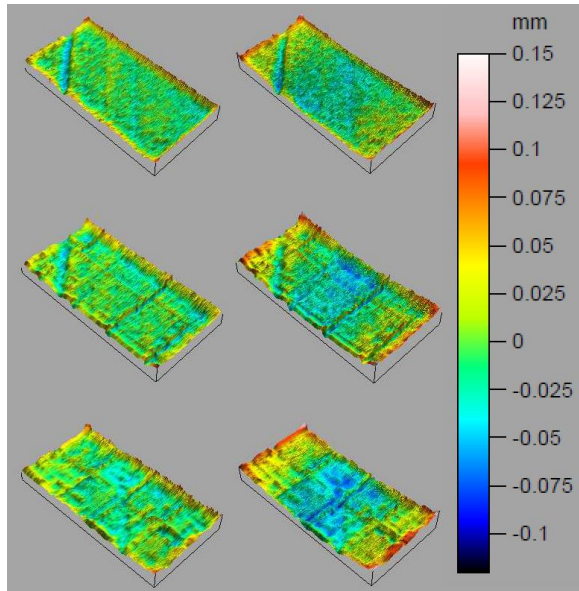


FIGURE 5. Surface Profilometry Results

Fig. 6 shows an example of the distortion seen in a centerline profile before and after removal (sample B3). Form calculation using a polynomial order 2 can characterize the shape of the bowing and gives an indication of the extent of distortion. The precision of the form calculation can be evaluated through comparison of the “before” profile and the “after” profile with the form removed – as shown in Fig. 7, this results in virtually identical profiles. The form profiles of 6 samples before- and- after being cut from the baseplate are shown in Fig. 8. The greatest distortion was observed in the

chess samples, followed by island and continuous. This is contrary to the hypothesis of chess generating lower distortions, as well as the measurements made by Kruth [3].

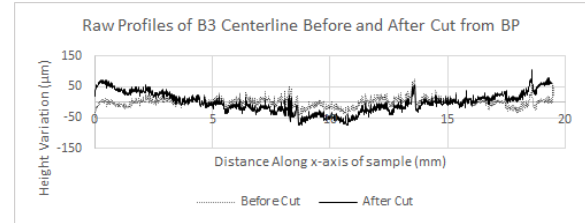


FIGURE 6. Sample B3 Centerline Profiles Before and After Sample was Cut from Baseplate

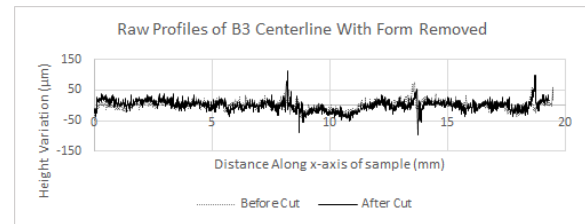


FIGURE 7. Sample B3 Centerline Profiles Before and After Sample was Cut from Baseplate – Form Removed from “After” profile

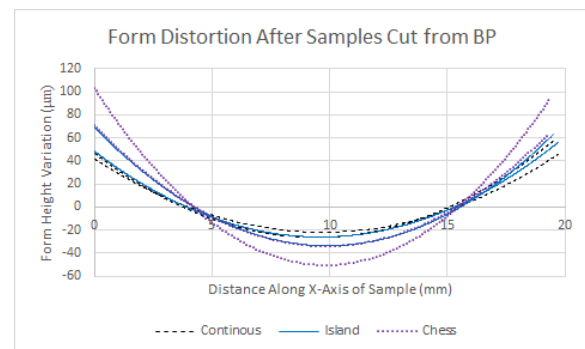


FIGURE 8. All Samples Cut from Baseplate - Form Distortion

To compare these distortions to Kruth’s [3], tangent lines were used to find the angle of distortion. Results are shown in Table 2. The profilometer data taken in this research clearly shows a different trend than that taken in Dr. Kruth’s, and the previous hypothesis that island and chess strategy consistently reduce distortion is shown to be incorrect.

TABLE 2. Measured Angles of Distortion

Sample	Measured Angle
Kruth 5mm Island (Ti64)	2.65°
Kruth Continuous (Ti64)	2.8°
A1: Continuous	1.54°
A2: Continuous	1.82°
B1: Island	1.82°
B2: Island	2.34°
C2: Chess	3.52°
C3: Chess	2.42°

Volumetric Residual Stress Measurements

The volumetric residual stress measurements showed the highest tensile stresses in the continuous sample, followed by island, and lowest in chess – see Figs. 9-11.

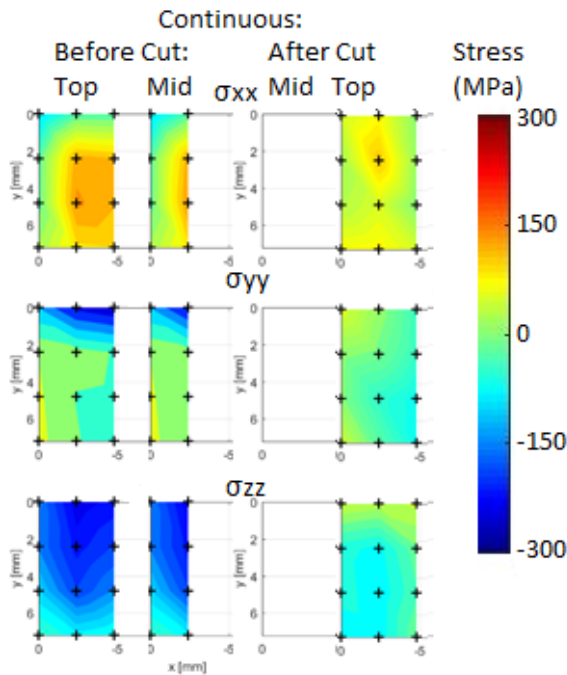


FIGURE 9. Continuous Sample (a) Before Removal and (b) After Removal

The anticipated x-direction tensile stresses are present when the samples are attached to the baseplate, and these stresses relieve significantly when the sample is removed and allowed to distort, to the point where they are very near zero for the chess sample.

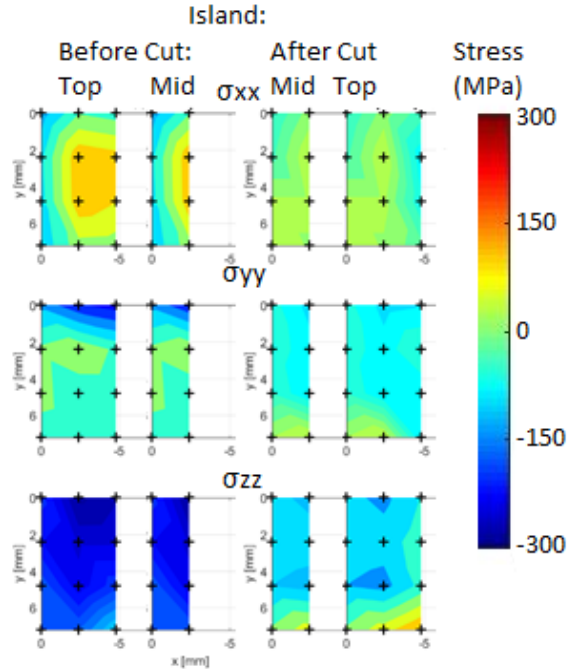


FIGURE 10. Island Sample (a) Before Removal and (b) After Removal

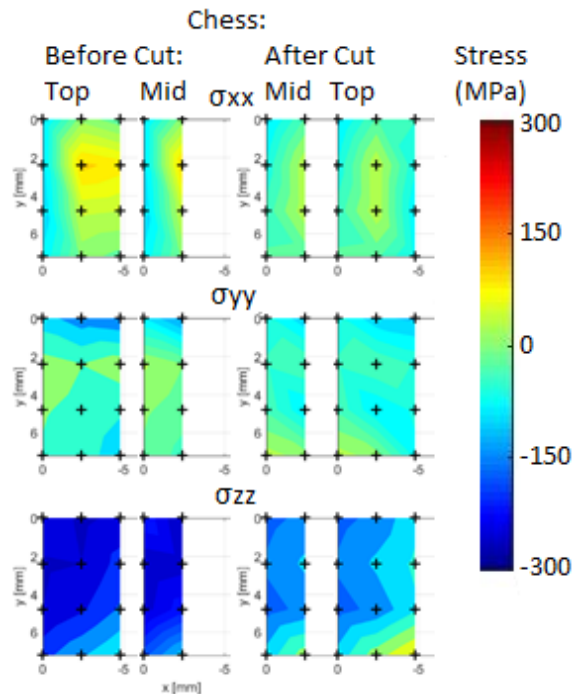


FIGURE 11. Chess Sample (a) Before Removal and (b) After Removal

High compressive stresses are seen in the z-direction, which is contrary to what was found in the initial study where z-direction stresses were tensile or close to zero. Once the sample is removed, these stresses are also relieved, but in this case the continuous sample nears zero stress while the chess and island samples retain some compressive stresses (with chess being highest in magnitude). This could be due to the stresses generated from the interlocking of the segments, which would not be relieved through sample removal and would be most severe in the chess sample.

CONCLUSION

Measurements clearly show the highest distortion (due to removal from the build plate and relieving residual stresses) in the chess sample, through evaluating both surface profilometry and a line scan down the center of the sample. This was not expected and inconsistent with previous work [3], and should be investigated further.

The tensile residual stresses in the x-direction were highest in the continuous sample, followed by island and chess, but the compressive residual stresses in the z-direction were highest in the chess sample, followed by island then continuous. This may be due to the binding nature of the segments.

FUTURE WORK

Although the shape of the arch lent itself to generation of higher residual stresses, the small size of the samples made volumetric measurement using neutron diffraction challenging. The smallest gage volume that could be reasonably utilized was 2 mm³, in order to have enough grains in the gage volume, and so the top of the arch could not be evaluated while ensuring gage volume burial. A similar shape but larger sample would be desirable to evaluate.

It is additionally recommended to conduct a follow-on study regarding build interruptions and their effect on residual stresses - the abnormal results from the initial study are likely due to the build interruption, since results from this study align closer with other residual stress research.

REFERENCES

[1] Sochalski-Kolbus LM, Payzant EA, Cornwell PA, Watkins TR, Babu SS, Dehoff RR, Duty C. Comparison of Residual Stresses in Inconel 718 Simple Parts Made by Electron Beam Melting and Direct Laser

- Metal Sintering. Metall. Mater. Trans. A. 2015; 1419-1432
- [2] Wu AS, Brown DW, Kumar M, Gallegos GF, King WE. An Experimental Investigation into Additive Manufacturing-Induced Residual Stresses in 316L Stainless Steel. Metall. Mater. Trans. A. 2014; 45.13: 6260-6270.
- [3] Kruth JP, Badrossamay M, Yasa E, Deckers J, Thijs L, Van Humbeeck J. Part and material properties in selective laser melting of metals. 16th International Symposium on Electromachining. 2010.
- [4] Mercelis P, Kruth JP. Residual stresses in selective laser sintering and selective laser melting. Rapid Prototyping Journal. 2006; 12.5: 254-265.
- [5] Gnäupel-Herold T, Slotwinski J, Moylan S. Neutron measurements of stresses in a test artifact produced by laser-based additive manufacturing. AIP Conf. Proc. 2014; 1581: 1205-12.
- [6] Kisi E, Howard C. Applications of Neutron Powder Diffraction. Oxford University Press, Oxford, UK. 2008; 420-438
- [6] Spooner S, Wang X. Diffraction peak displacement in residual stress samples due to partial burial of the sampling volume. J. Appl. Crystallogr. 1997; 30: 449-455.